Supplementary material for "Effects of mesozooplankton growth and reproduction on plankton and organic carbon dynamics in a marine biogeochemical model"

Corentin Clerc[1,2], Laurent Bopp[2], Fabio Benedetti[1], Nielja Knecht[1,3], Meike Vogt[1], and Olivier Aumont[4]

[1]Environmental Physics, Institute of Biogeochemistry and Pollutant Dynamics, ETH Zürich, 8092, Zürich, Switzerland.
[2]LMD / IPSL, Ecole normale supérieure / Université PSL, CNRS, Ecole Polytechnique, Sorbonne Université, Paris, France
[3]Stockholm Resilience Center Stockholm University, Stockholm, Sweden
[4]LOCEAN / IPSL, IRD, CNRS, Sorbonne Université, MNHN, Paris, France

Correspondence: Corentin Clerc (corentin.clerc@usys.ethz.ch)

Model	$RMSE_{Train}$	$RMSE_{Test}$	r^2_{Train}	r^2_{Test}	NSE_{Train}	NSE_{Test}
GLM	0.26	0.35	0.38	-0.09	0.38	0.38
GAM	0.26	0.27	0.36	0.36	0.36	0.36
RF	0.23	0.23	0.51	0.52	0.82	0.52
GBM	0.18	0.24	0.70	0.48	0.64	0.48
DL	0.25	0.26	0.41	0.40	0.41	0.40

Table S1. Performance for the mesozooplankton biomass distribution models (BDMs-MAREDAT). Each model metric was calculated on both the training set (X_{train}) and the testing set (X_{test}). r^2 ranges from -∞ to +1, with a perfect fit of the model and full variance explained indicated by a value of +1. The root mean squared error (RMSE) is an error measure, hence smaller values show higher accuracy. The Nash-Sutcliffe-efficiency (NSE) indicates improvement of the model predictions over using the observation mean, with perfect model performance indicated by a value of +1 and a value of 0 indicating that the models perform no better than the observation mean.

Random forest

Hyperparameter	Parameter values tested	Final parameter
ntree	100, 300, 1000	100
mtry	1, 7	7
minrows	1, 10	1
max depth	10, 20	20
sample	1	1

Gradient Boosting Machine

Hyperparameter	Parameter values tested	Final parameter
max depth	1, 3, 5	1
minrows	1, 10	10
rlearn	0.01, 0.1	0.01
rsample	1	1
rsamplecolumns	1	1

Deep Learning

Hyperparameter	Parameter values tested	Final parameter
activation function	tanh	tanh
hidden layer structure	(5;5), (20;20)	(20;20)
λ (L1)	0, 1e-3, 1e-5	1e-5
λ (L2)	0, 1e-3, 1e-5	1e-3

Table S2. Hyperparameter options for the Random Forest (RF), the Gradient Boosting Machine (GBM) and the Deep Learning (DL) models. For each algorithm, the final hyperparameter choices for the BDM-MAREDAT field was determined via a grid search by assessing all hyperparameter options for those that would minimise the root mean squared error (RMSE). For the RF: ntree denotes the number of bootstrap samples created from the original dataset, using a fraction of rsample of the entire data for each bootstrap. mtry refers to the number of predictors evaluated at each node for their ability to discriminate the data most clearly. minrows describes the minimum number of observations in each terminal node and maxdepth the maximum size of the tree. For the GBM: maxdepth describes the maximum size of each individual tree and minrows denotes the minimum number of observations in each terminal node. The model's learning rate is determined by rlearn. Each of the individual trees that together make up the GBM is trained on a a random fraction rsample of the data, using a fraction rsamplecolumns of the predictors. For the DL: The activation function describes the non-linear transformation applied at each neuron. The hidden layer structure determines the number of layers and the number of neurons per layer, e.g. (10, 10) denotes a network with two hidden layers of ten neurons each. λ (L1) and λ (L2) are weight parameters used to penalise complexity. To avoid overfitting, L1 (Lasso regression) or L2 (Ridge regression) can be employed to add a penalty term based on the network weights. The strength of this penalising factor is determined by the respective parameter λ. For an extensive description of all hyperparameters, refer to Boehmke and Greenwell (2019).

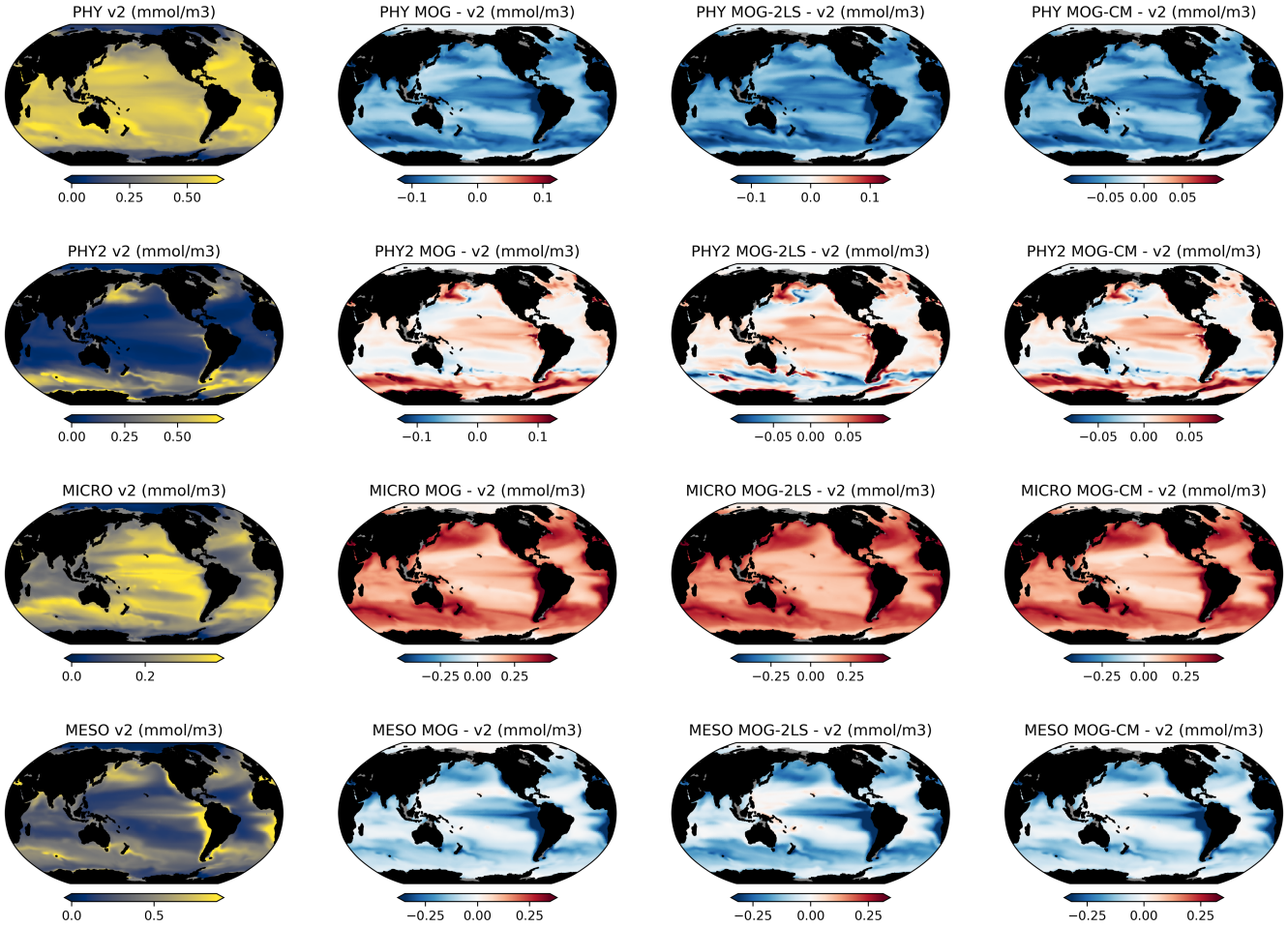

Figure A1. Phyto- and zooplankton biomasses as simulated by PISCES-v2 and anomalies with PISCES-MOG, PISCES-MOG-2LS and PISCES-MOG-CM. A complete description of the different model versions in available in section 2.2.2 of the methods

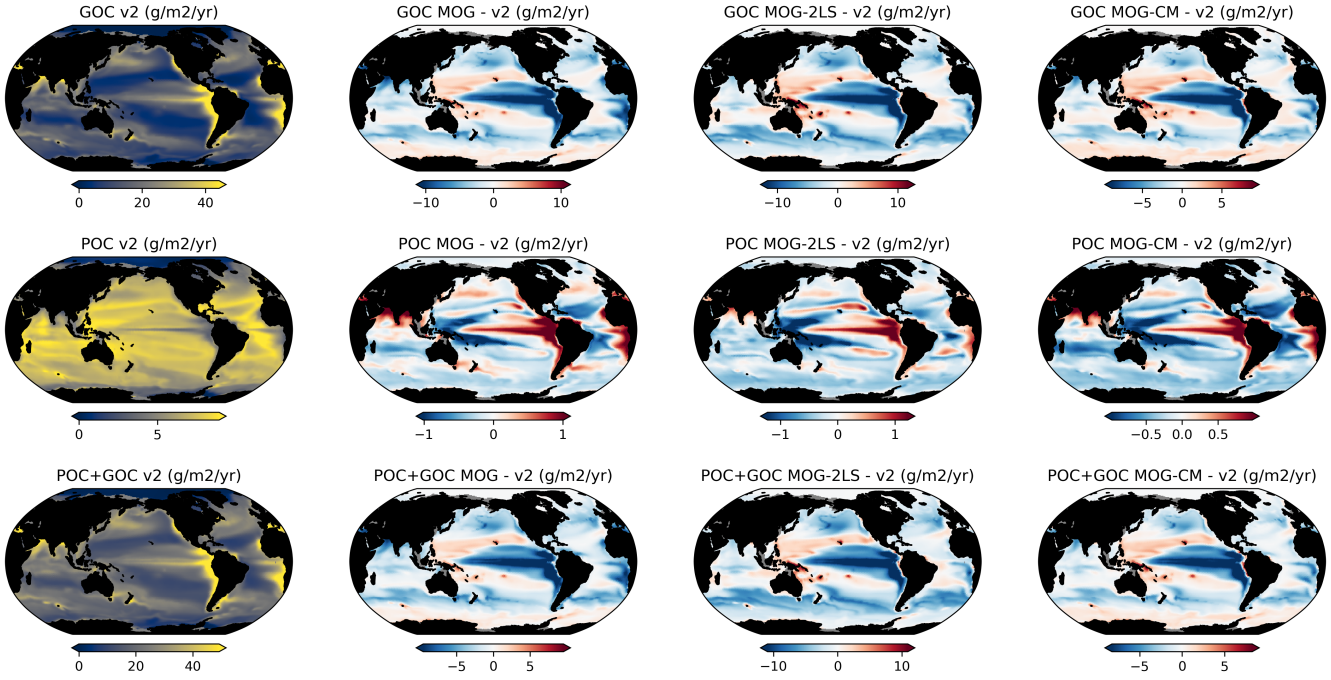

Figure A2. Small, large and total particulate carbon export as simulated by PISCES-v2 and anomalies with PISCES-MOG, PISCES-MOG-2LS and PISCES-MOG-CM. A complete description of the different model versions in available in section 2.2.2 of the methods. POC refers to small POC, GOC refers to large POC and POC+GOC refers to the total particulate carbon fluxes.

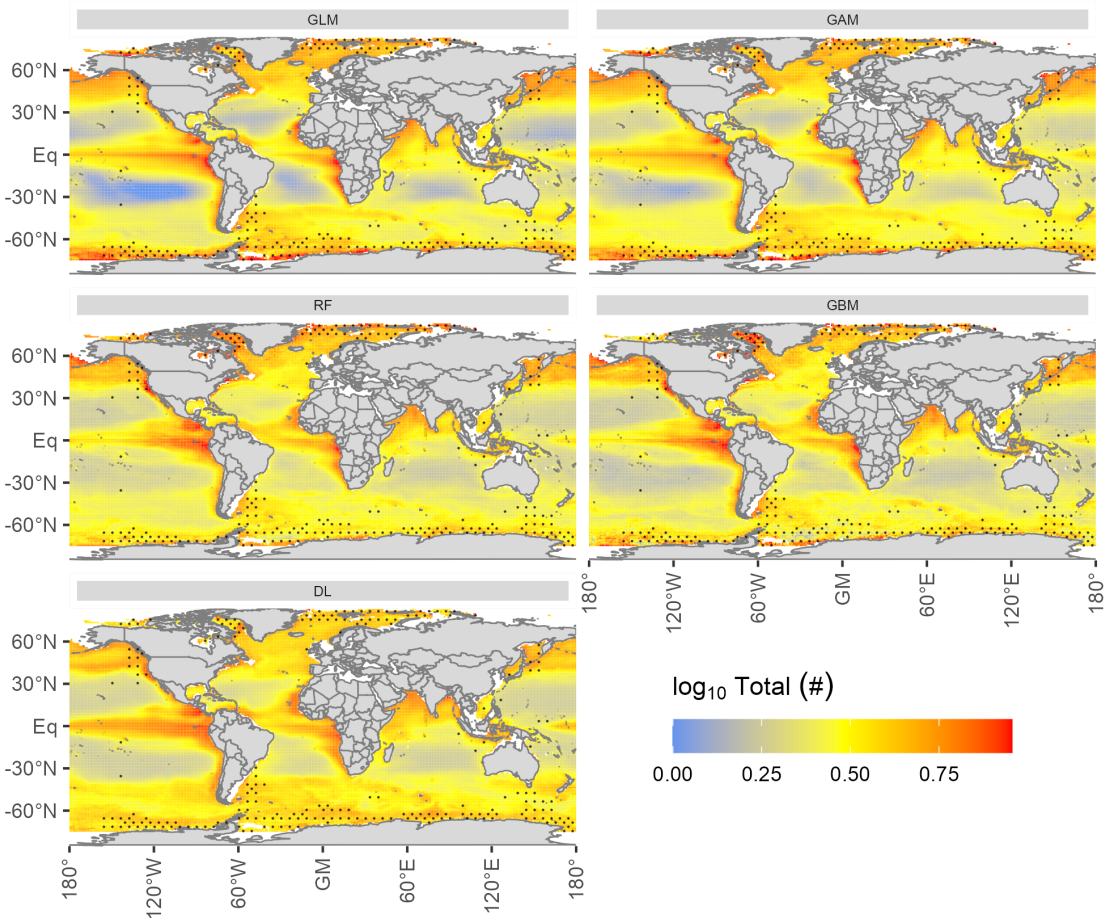

Figure A3. Mean annual mesozooplankton biomass predictions as calculated by the five different models. Values are shown as log10(x + 1). Stippled areas indicate grid points where the environmental conditions were outside the training dataset for more than six months of the year as calculated with the Multivariate Environmental Similarity Surfaces (MESS) analysis.

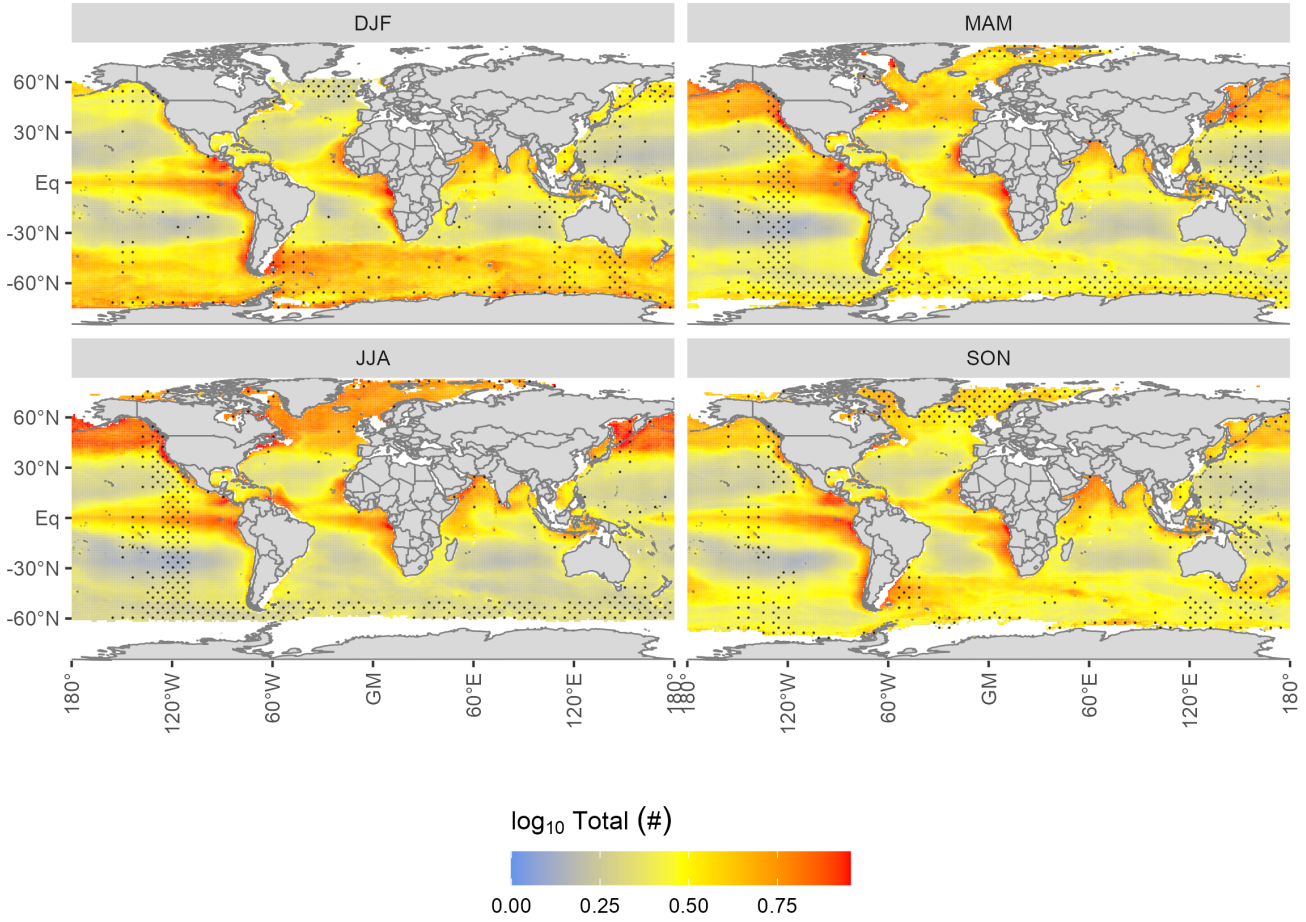

Figure A4. Seasonal mean mesozooplankton biomass predictions as mean over the five models (DJF = December - February, MAM = March - May, JJA = June - August, SON = September - November). Values are shown as log10(x + 1). Stippled areas indicate grid points where the environmental conditions were outside the training dataset for more than one month of the respective season as calculated with the Multivariate Environmental Similarity Surfaces (MESS) analysis.

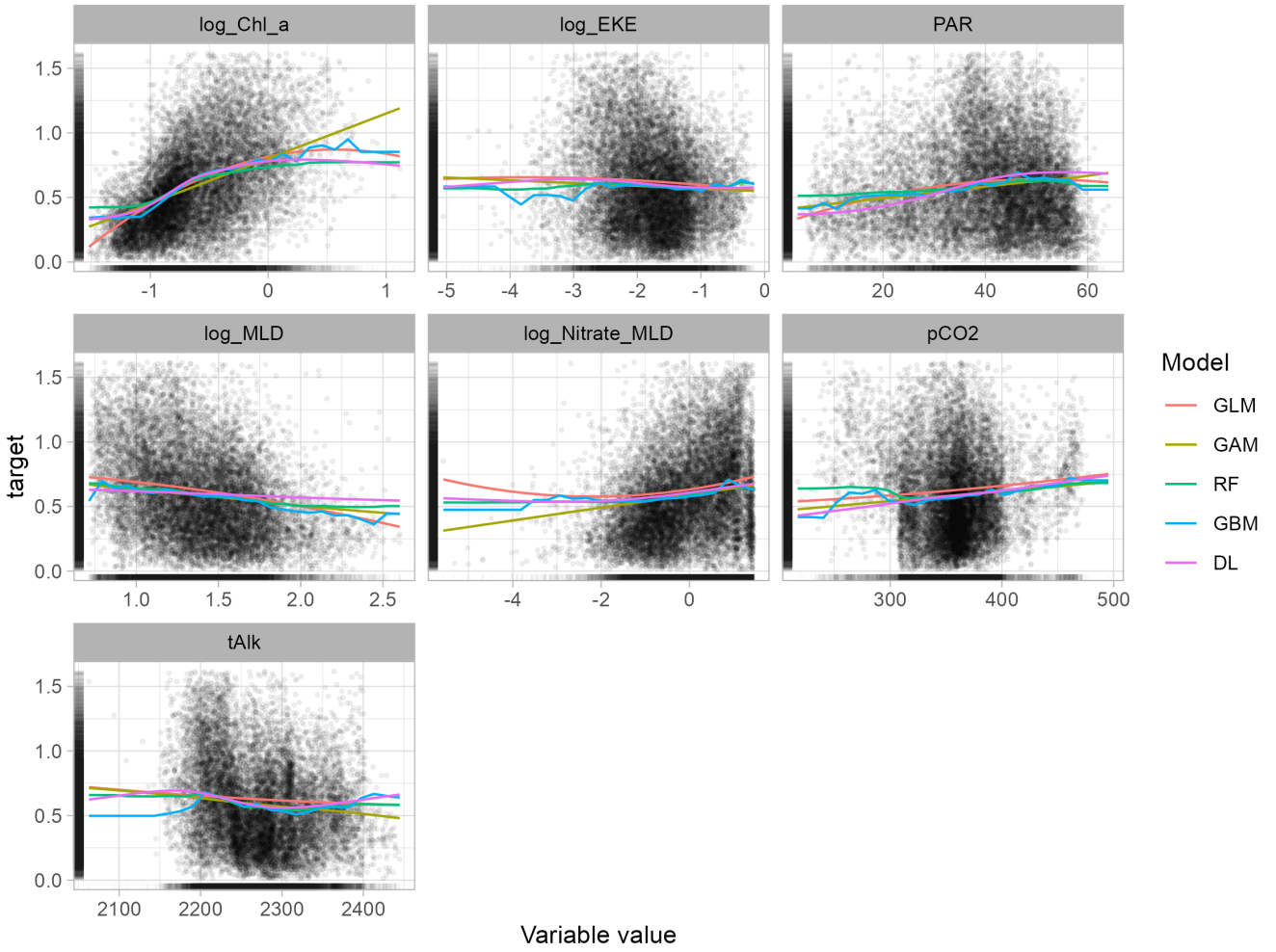

Figure A5. Partial dependence plots (PDP) for the environmental predictors biomass distribution models (BDMs). The curves indicate the relations learned by the different BDMs and the rug on the x- and y-axis represents the distribution of the training data. MLD refers to the mixed layer depth, EKE to the eddy kinetic energy. The different model types are the Generalized Linear Model (GLM), Generalized Additive Model (GAM), Random Forest (RF), Boosted Regression Tree (GBM) and Neural Network (DL).

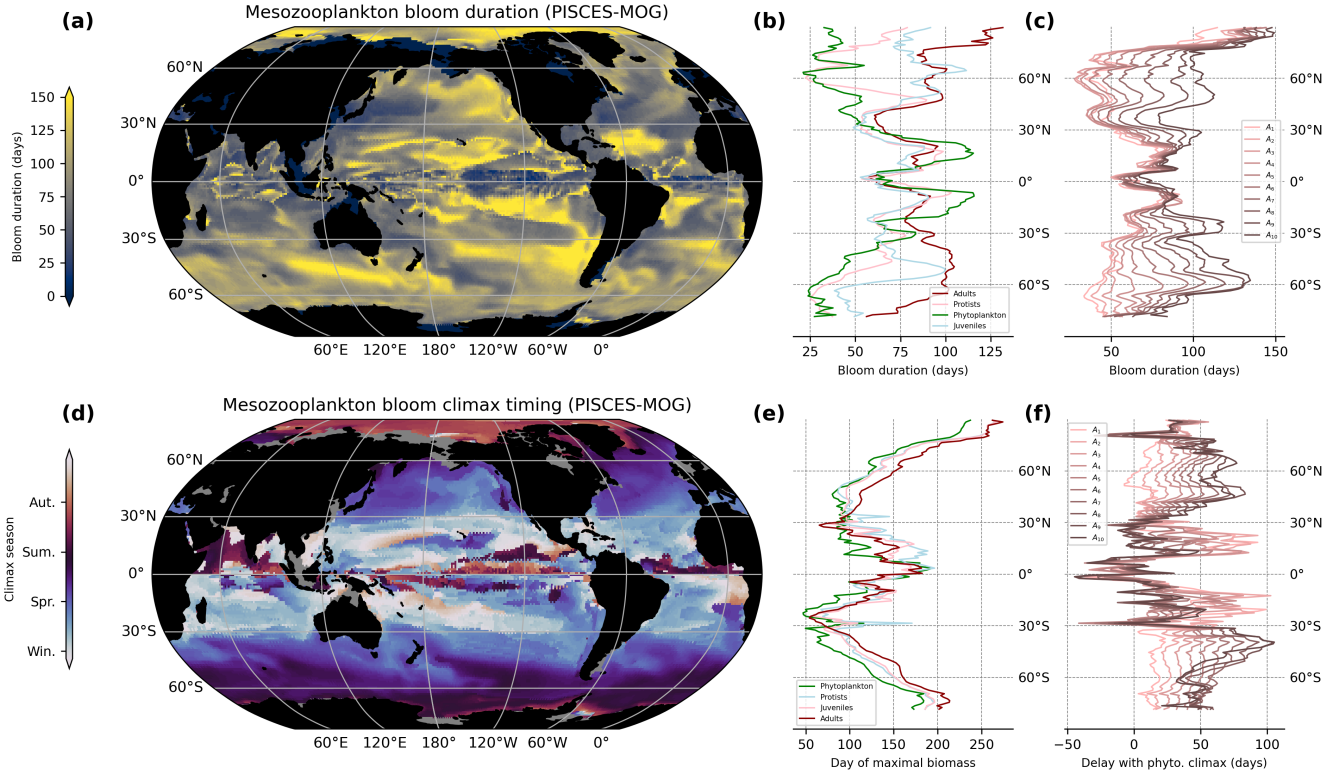

Figure A6. Global and zonally averaged mesozooplankton bloom duration and climax(a) Global average of simulated (by PISCES-MOG) epipelagic (0-200m) mesozooplankton bloom duration (days spent within the 75th quantile of the yearly seasonal cycle) . (b) Zonal mean of adult (red) and juvenile (pink) metazoans, unicellular protists (light blue), and total phytoplankton (green) bloom duration (days). (c) Mean zonal bloom duration for the 10 adult metazoans size-classes simulated in PISCES-MOG. (d) Global average of simulated (by PISCES-MOG) epipelagic (0-200m) mesozooplankton bloom climax (day of maximal population growth) . (b) Zonal mean of adult (red) and juvenile (pink) metazoans, unicellular protists (light blue), and total phytoplankton (green) bloom climax (day of year). (f) Mean zonal delay (days) between bloom climax for the 10 adult metazoans size-classes and bloom climax for phytoplankton as simulated in PISCES-MOG.

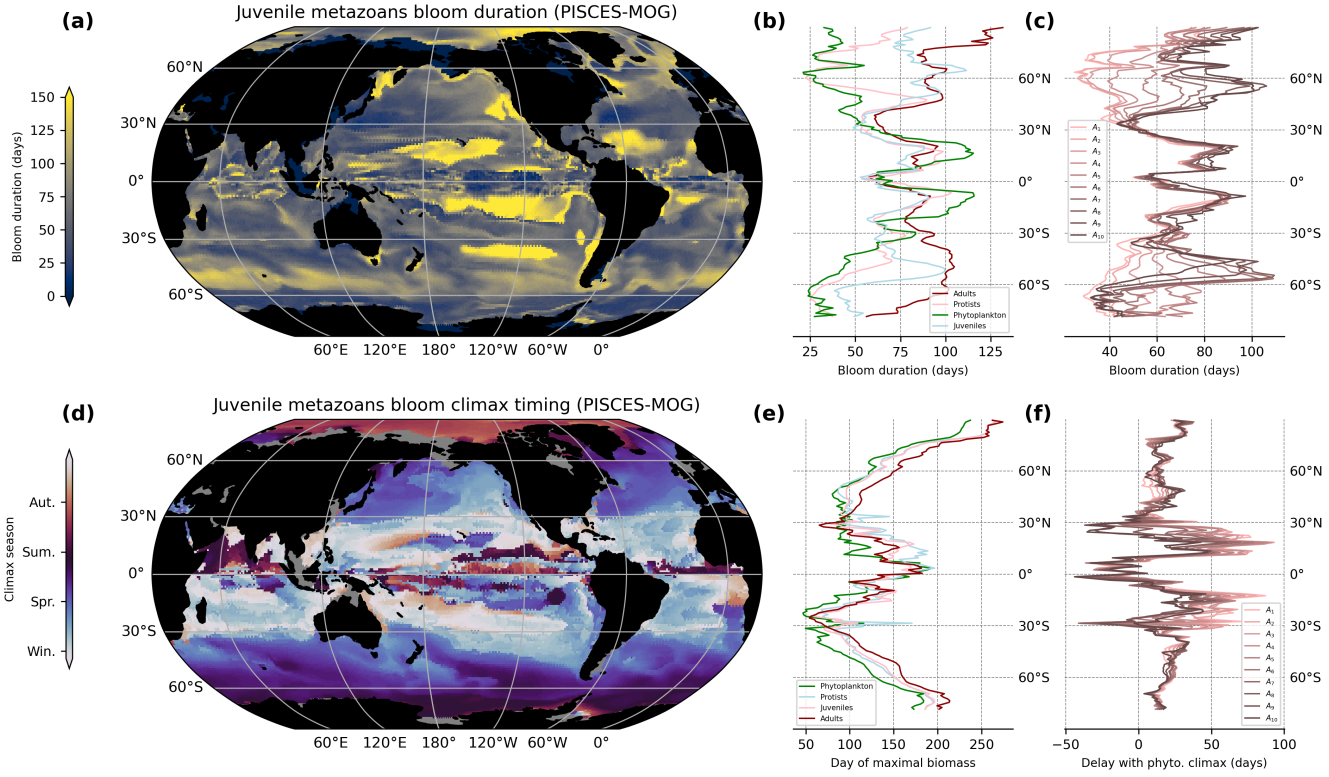

Figure A7. Global and zonally averaged juvenile metazoans bloom duration and climax (a) Global average of simulated (by PISCES-MOG) epipelagic (0-200m) juvenile metazoans bloom duration (days spent within the 75th quantile of the yearly seasonal cycle) . (b) Zonal mean of adult (red) and juvenile (pink) metazoans, unicellular protists (light blue), and total phytoplankton (green) bloom duration (days). (c) Mean zonal bloom duration for the 10 juvenile metazoans size-classes simulated in PISCES-MOG. (d) Global average of simulated (by PISCES-MOG) epipelagic (0-200m) juvenile metazoans bloom climax (day of maximal population growth) . (b) Zonal mean of adult (red) and juvenile (pink) metazoans, unicellular protists (light blue), and total phytoplankton (green) bloom climax (day of year). (f) Mean zonal delay (days) between bloom climax for the 10 juvenile metazoans size-classes and bloom climax for phytoplankton as simulated in PISCES-MOG.

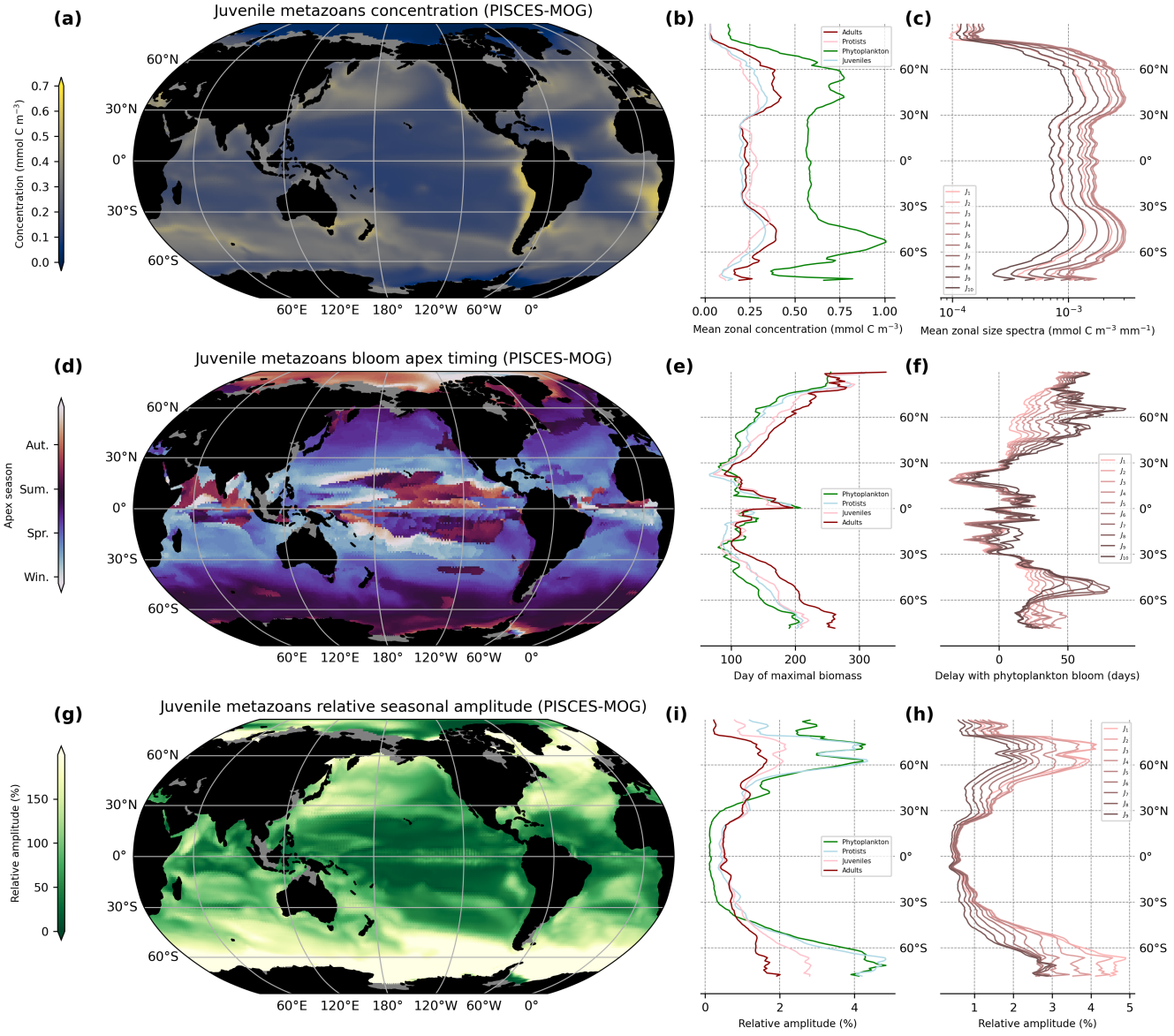

Figure A8. Global and zonally averaged epipelagic (0-200 m) plankton biomass and seasonality simulated by PISCES-MOG (a) Global average of epipelagic juvenile metazoan concentration (mmol C m^{-3}). (b) Zonal mean of adult (red) and juvenile (pink) metazoans, unicellular protists (light blue), and total phytoplankton (green) concentrations (mmol C m^{-3}). (c) Mean zonal size spectra (biomass over size class width, mmol C m^{-3} mm^{-1}) for the 10 juvenile metazoans size-classes. (d) Global average of epipelagic juvenile metazoans bloom apex (day of maximal abundance). (e) Zonal mean plankton groups bloom apexes (days, same colors as above) (f) Mean zonal delay (days) between the bloom apex of the 10 juvenile metazoans size classes and the bloom apex of phytoplankton. (g) Global average of epipelagic juvenile metazoans relative seasonal amplitude (%) (h) Zonal mean plankton groups relative seasonal amplitude (%, same colors as above). (i) Mean zonal relative seasonal amplitude (%) for the 10 juvenile metazoans size-classes.

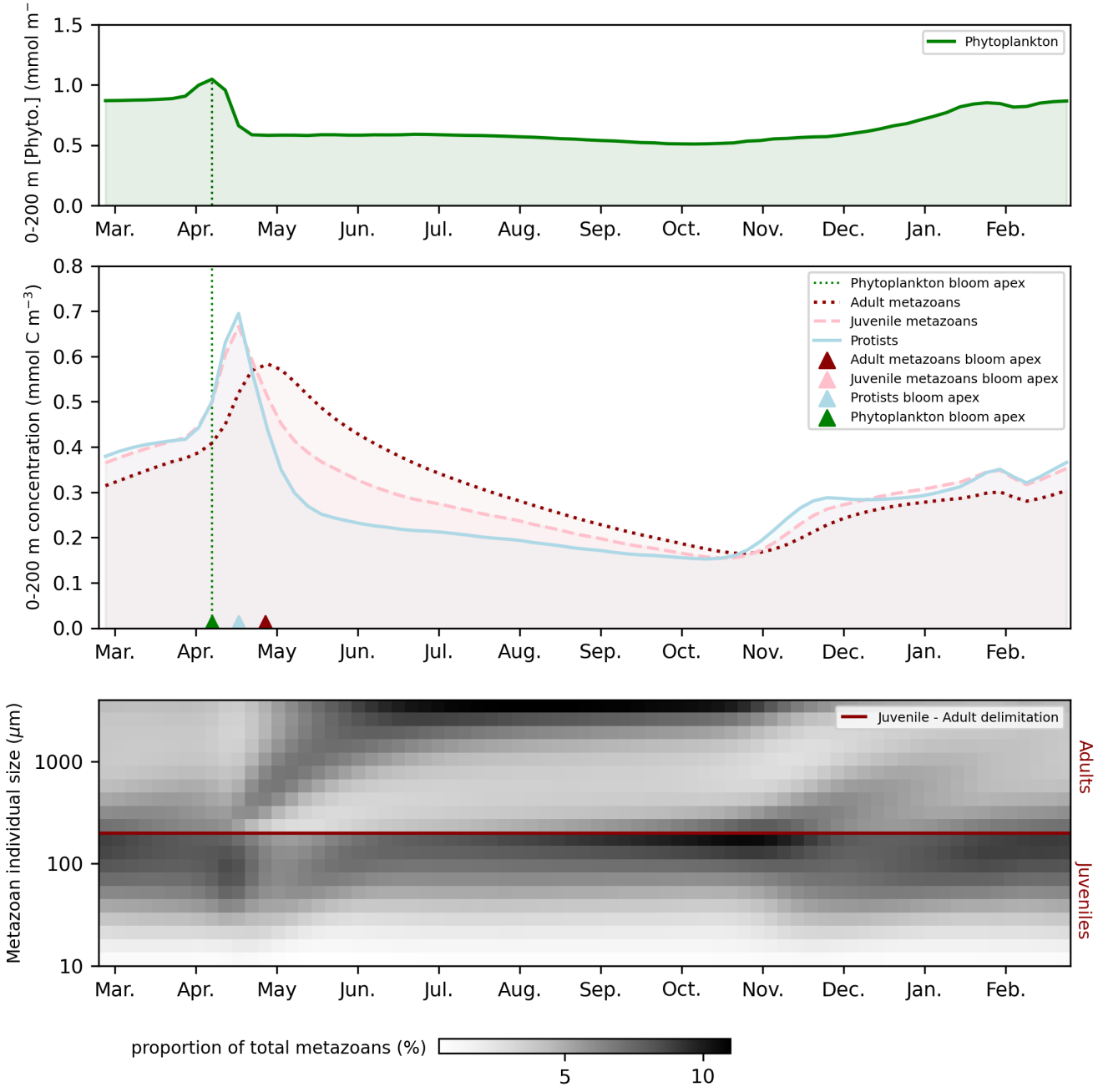

Figure A9. Seasonal dynamics of the epipelagic (0-200 m) ecosystem simulated by PISCES-MOG at BATS location. The coordinates are chosen to match the location of the BATS time-series (see section 2.3.2). Time evolution of (a) the phytoplankton and (b) the zooplankton concentrations (mmol C m^{-3}) over one year. Triangles indicate the bloom apexes of the plankton groups. (c) Change in size-class composition of metazoans over the year. The y-axis represent the 20 size classes ordered by increasing size. The grey levels correspond to the proportion of total metazoans (juvenile + adults) in each size classes for each time-step. Thus, for each time step, the proportions of the 20 size classes sums to 100. The arrows indicate cohorts, namely the propagation of successive waves of biomass from small to large organisms.

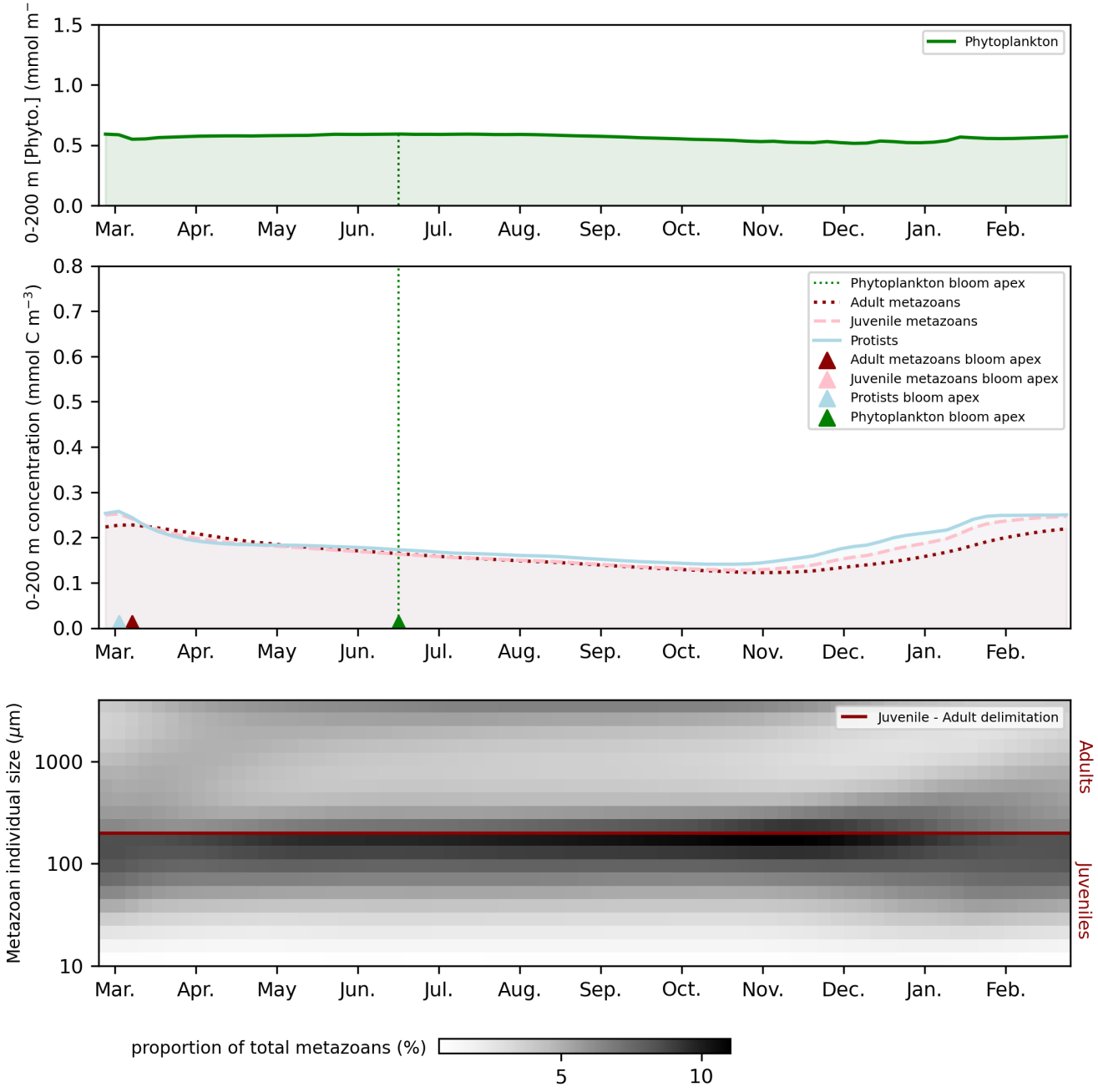

Figure A10. Seasonal dynamics of the epipelagic (0-200 m) ecosystem simulated by PISCES-MOG at HOT location. The coordinates are chosen to match the location of the HOT time-series (see section 2.3.2). Time evolution of (a) the phytoplankton and (b) the zooplankton concentrations (mmol C m^{-3}) over one year. Triangles indicate the bloom apexes of the plankton groups. (c) Change in size-class composition of metazoans over the year. The y-axis represent the 20 size classes ordered by increasing size. The grey levels correspond to the proportion of total metazoans (juvenile + adults) in each size classes for each time-step. Thus, for each time step, the proportions of the 20 size classes sums to 100. The arrows indicate cohorts, namely the propagation of successive waves of biomass from small to large organisms.

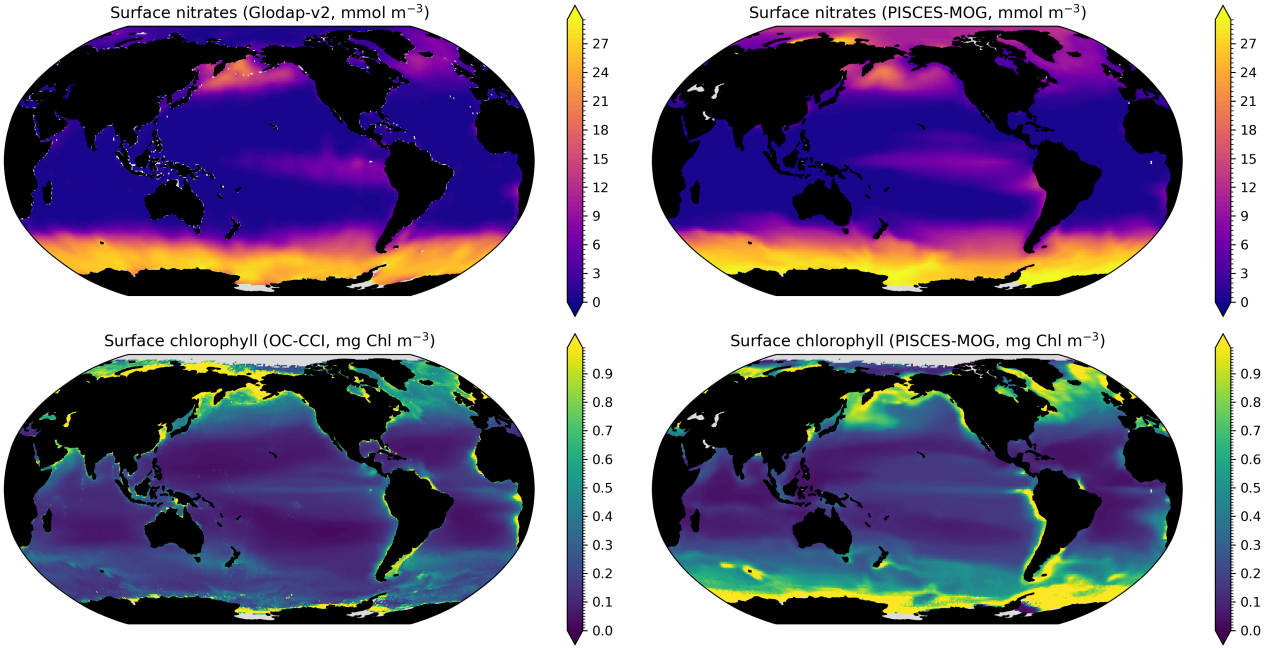

Figure A11. Comparison between modeled and observed annual average surface nitrates (a, b), surface chlorophyll (c, d) NO3 surface fields from the World Ocean Atlas (Garcia et al., 2019) are used to evaluate our modeled nutrient distributions. The long-term multi-sensor time series OC-CCI (Ocean Colour project of the ESA Climate Change Initiative; Sathyendranath et al., 2019) for satellite phytoplankton chlorophyll a sea surface concentration converted into mg Chl m-3 is used to evaluate our modeled total chlorophyll distribution. The model performs particularly well for surface nitrates, with absolute values and simulated spatial patterns very consistent with observations ($r_{spearman}$ = 0.75). The correspondence between the observed and simulated surface chlorophyll is rather satisfactory ($r_{spearman}$ = 0.65). The average value is similar (0.35 vs. 0.33 mg Chl m-3), and the spatial structure is respected overall. The overall variability is of the same order of magnitude in the model and the observations (standard deviation of 0.97 mg Chl m^{-3} for the observations and 0.37 mg Chl m^{-3} for the model). However, there are some differences. At high latitudes, particularly in the Southern Ocean, the model tends to overestimate chlorophyll compared to the satellite product. However, satellite chlorophyll may be underestimated by a factor of about 2 to 2.5 by the algorithms deducing chlorophyll concentrations from reflectance, as discussed in Aumont et al. (2015).

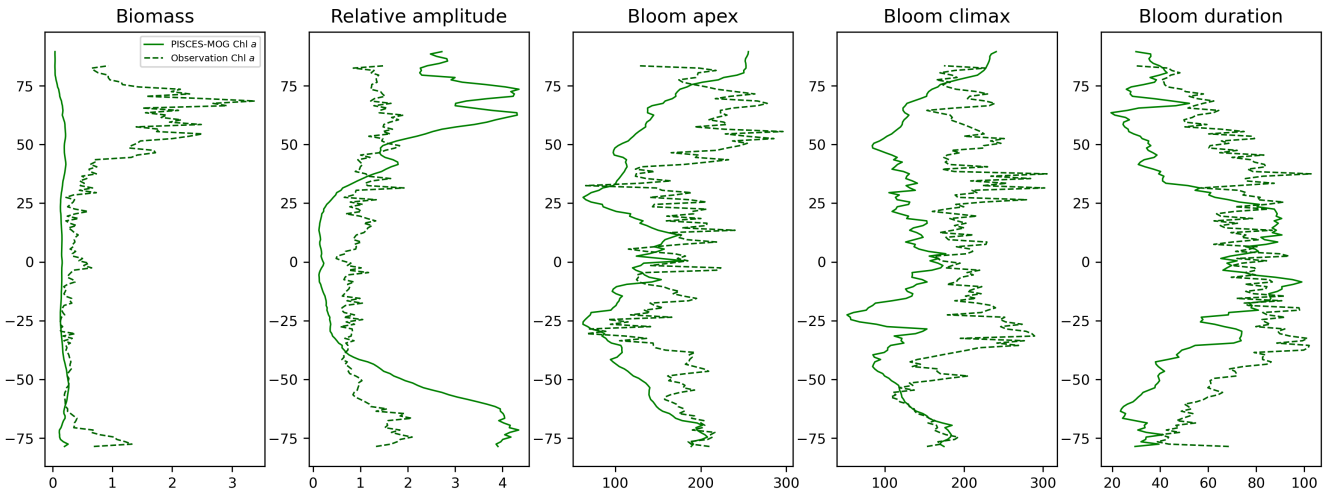

Figure A12. Model-data comparison of the chlorophyll-a concentrations and seasonality. For each of the five evaluated metrics, we compare the zonal mean of the metric computed on the chlorophyll distribution simulated by PISCES-MOG (plain line) and from satellite observation (dotted line). The five metrics evaluated are (a) concentration (mg Chl m^{-3}), (b) relative seasonal amplitude (%), (c) bloom apex (day of the year), (d) bloom climax (day of the year) and (e) bloom duration (days). The metrics are defined is the methods section **??**

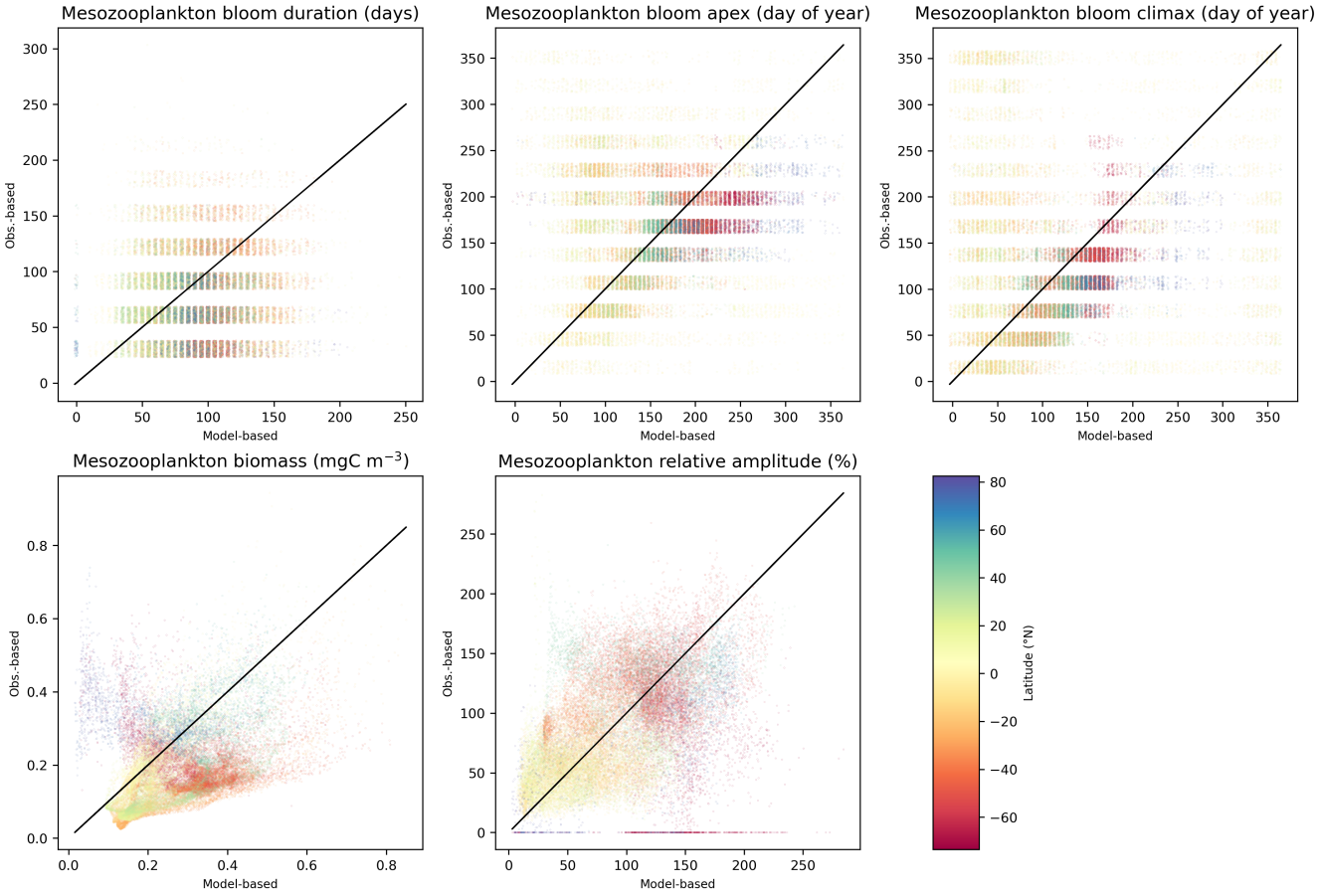

Figure A13. Model-observation comparison for five mesozooplankton metrics. The ordinate represents the metric value computed from the observation-based BDMs-MAREDAT field, while the abscissa represents the metric value computed from the PISCES-MOG simulations. The compared metric is indicated at the top of each subplot. Note that for bloom apex, climax, and duration, uniform noise was added to each (x, y) value to prevent overlapping of multiple points. Thus, each rectangle corresponds to a single point.

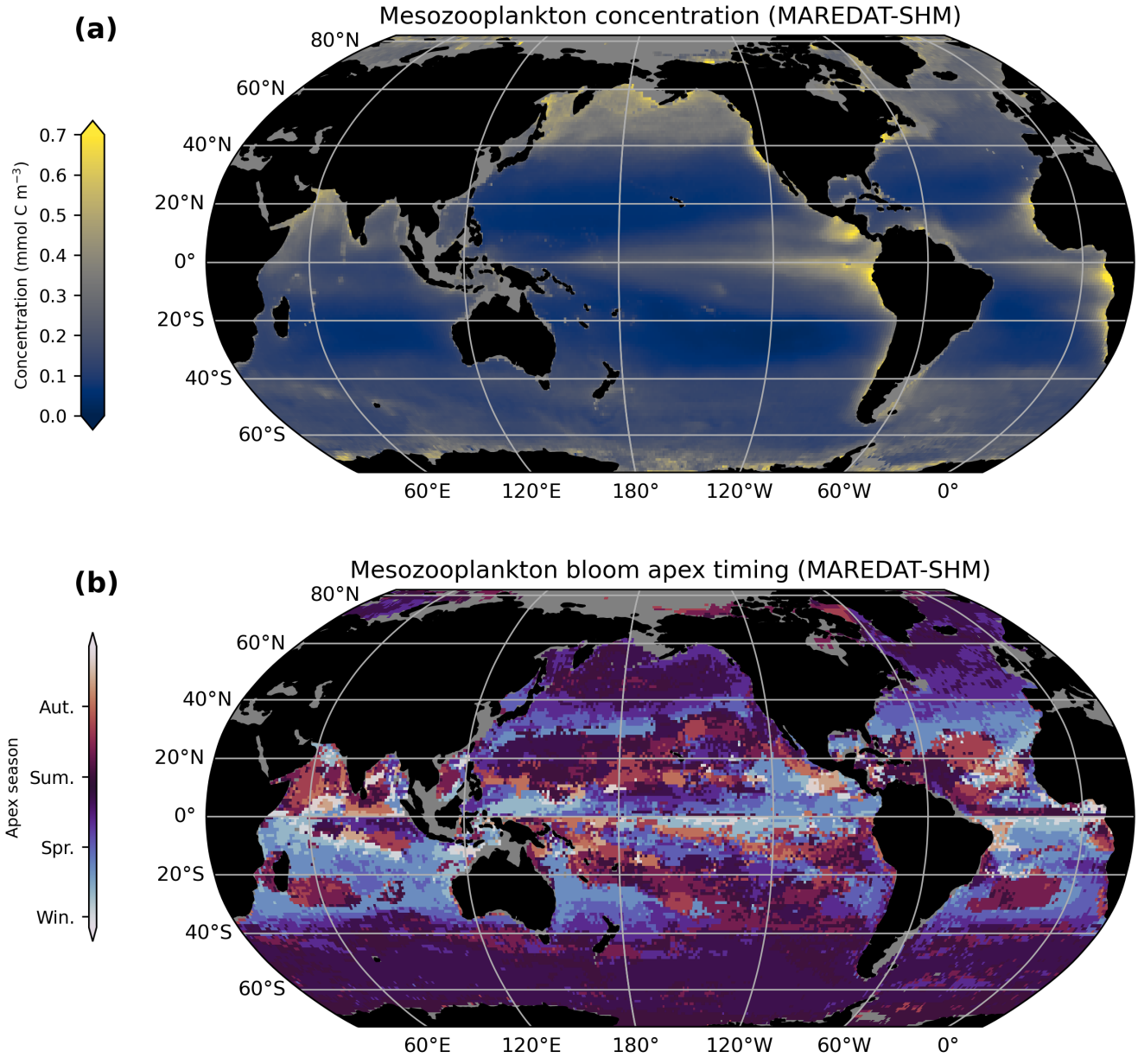

Figure A14. Interpolated global averaged mesozooplankton biomass and bloom apex from field observations (a) Global average of BDMs-MAREDAT epipelagic (0-200m) epipelagic (0-200m) mesozooplankton concentration (mmol C m^{-3}) (d) Global average of BDMs-MAREDAT epipelagic (0-200m) mesozooplankton bloom apex (day of maximal population growth)

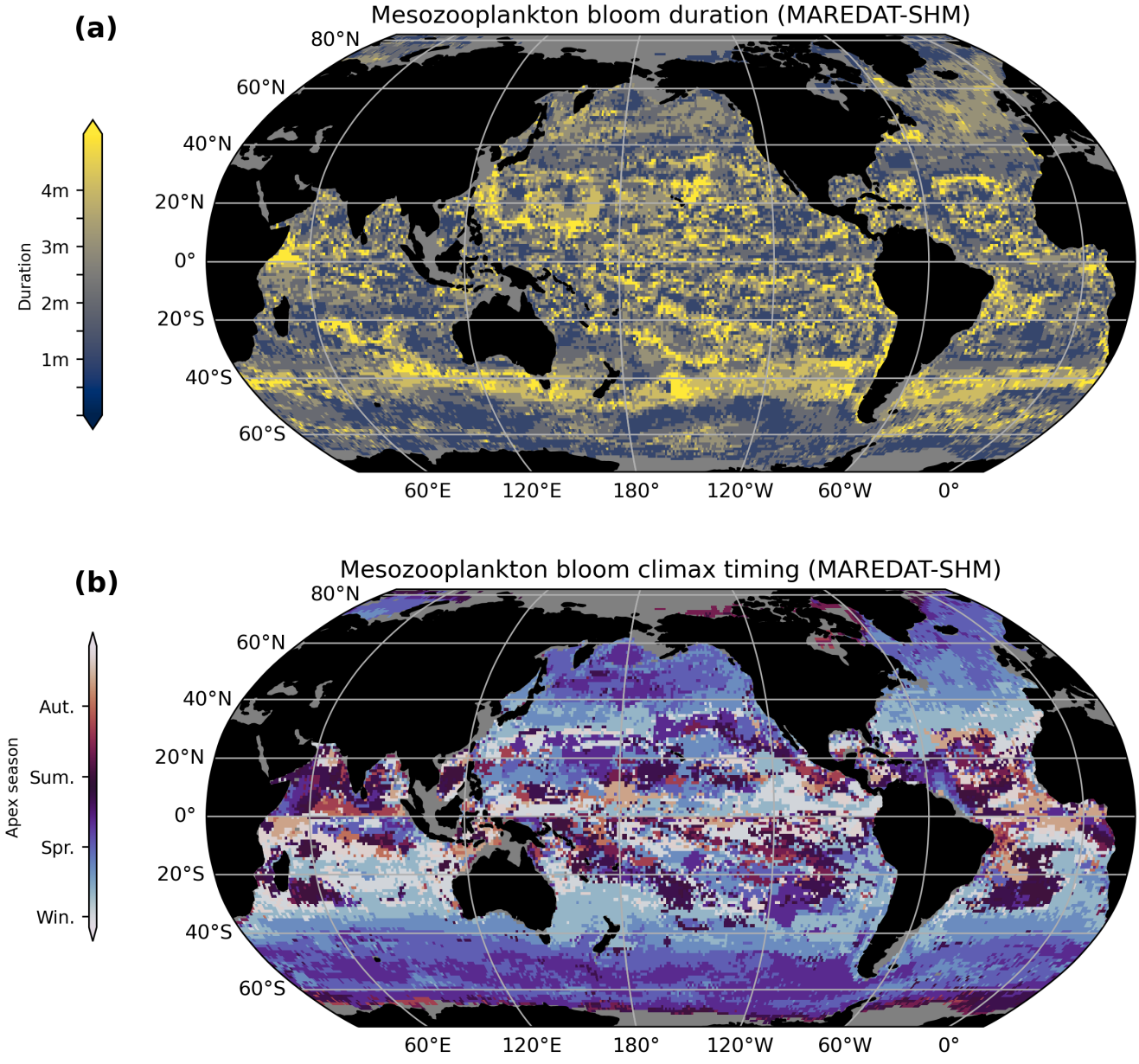

Figure A15. Interpolated global averaged mesozooplankton bloom duration and climax from field observations (a) Global average of BDMs-MAREDAT epipelagic (0-200m) mesozooplankton bloom duration (days spent within the 75th quantile of the yearly seasonal cycle) (d) Global average of BDMs-MAREDAT epipelagic (0-200m) mesozooplankton bloom climax (day of maximal population growth)

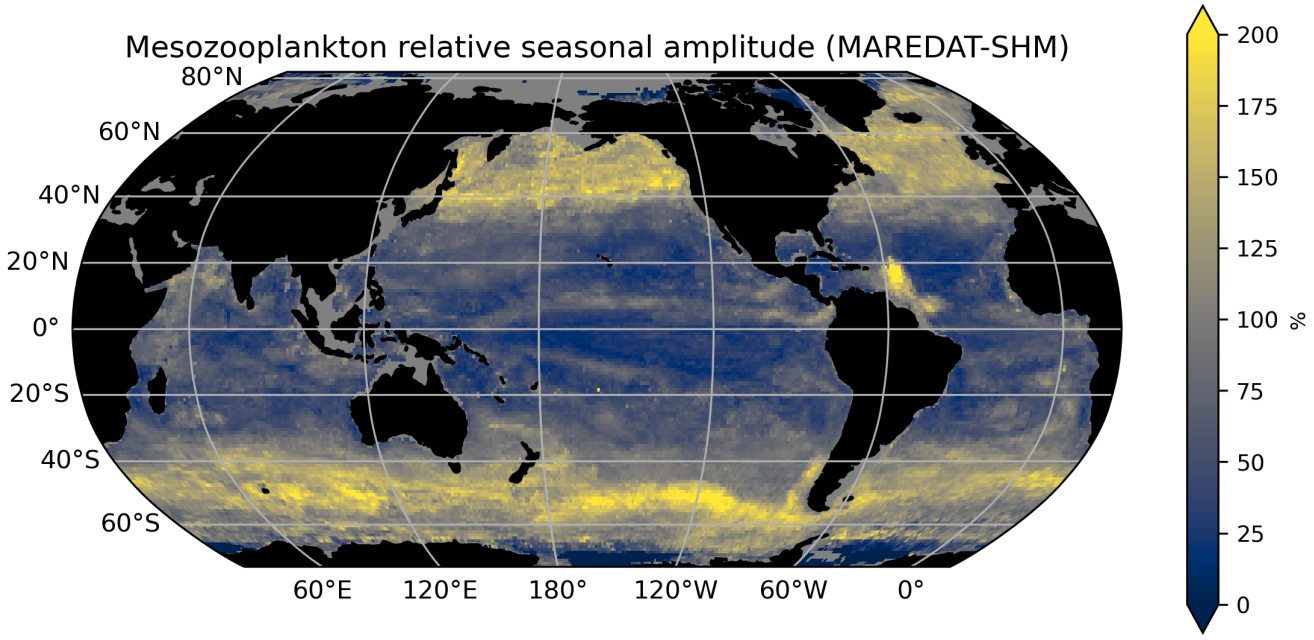

Figure A16. Interpolated global averaged mesozooplankton relative seasonal amplitude from field observations Global average of BDMs-MAREDAT epipelagic (0-200m) epipelagic (0-200m) mesozooplankton relative seasonal amplitude (%)

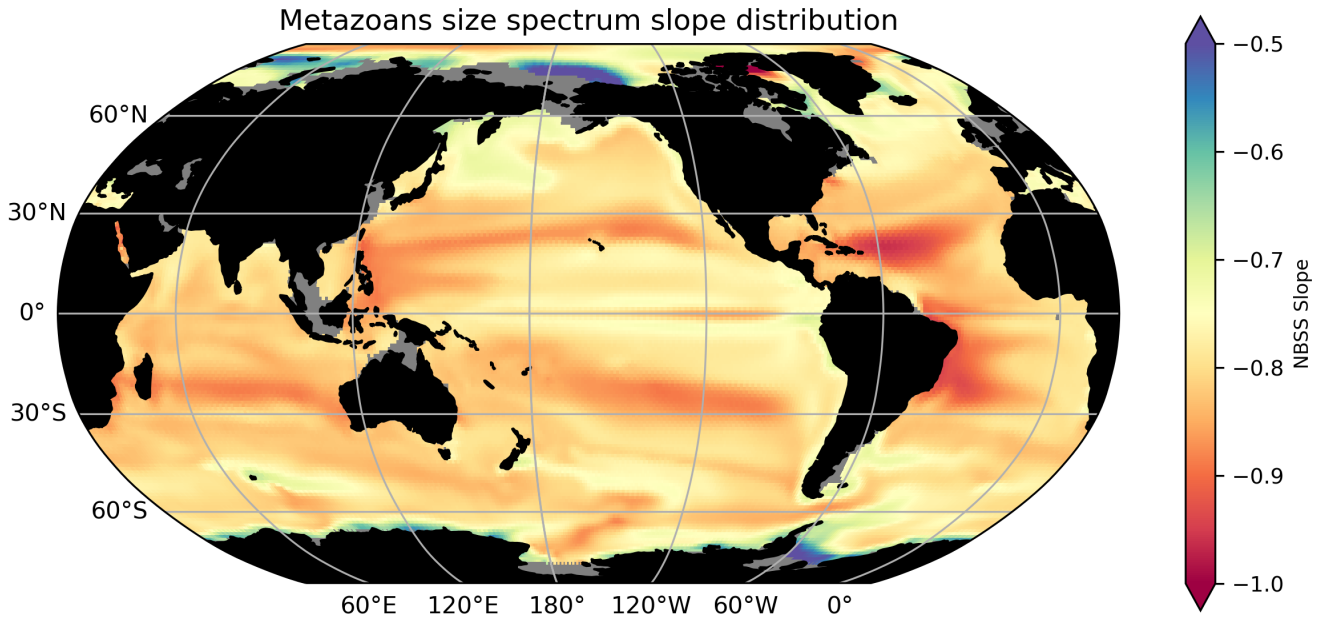

Figure A17. Metazoans Normalized Biomass Size Spectrum (NBSS) slope distribution. To compute the NBSS slope in each grid cell, we fitted a linear model between the log-transformed normalized biomasses of the 20 metazoan sizes classes (concentration over the top 200 m divided by the width of the size class) and the log transformed geometrical mean size of the size classes. The resulting slope of the linear regression is the NBSS slope.